Citation: Xu, P., L. Li, F. Zhang, G. Stephanopoulos, and M. Koffas. "Improving Fatty Acids Production by Engineering Dynamic Pathway Regulation and Metabolic Control." Proceedings of the National Academy of Sciences 111, no. 31 (July 21, 2014): 11299–11304. © 2014 National Academy of Sciences

As Published: http://dx.doi.org/10.1073/pnas.1406401111

Publisher: National Academy of Sciences (U.S.)

Persistent URL: http://hdl.handle.net/1721.1/95755

Version: Final published version: final published article, as it appeared in a journal, conference proceedings, or other formally published context

Massachusetts Institute of Technology

Improving fatty acids production by engineering dynamic pathway regulation and metabolic control

Peng Xu[a,b], Lingyun Li[b,c], Fuming Zhang[a,b], Gregory Stephanopoulos[d], and Mattheos Koffas[a,b,c,1]

[a]Department of Chemical and Biological Engineering, Rensselaer Polytechnic Institute, Troy, NY 12180; [b]Center for Biotechnology and Interdisciplinary Studies, Rensselaer Polytechnic Institute, Troy, NY 12180; [c]Department of Biological Sciences, Rensselaer Polytechnic Institute, Troy, NY 12180; and [d]Department of Chemical Engineering, Massachusetts Institute of Technology, Cambridge, MA 02139

Global energy demand and environmental concerns have stimulated increasing efforts to produce carbon-neutral fuels directly from renewable resources. Microbially derived aliphatic hydrocarbons, the petroleum-replica fuels, have emerged as promising alternatives to meet this goal. However, engineering metabolic pathways with high productivity and yield requires dynamic redistribution of cellular resources and optimal control of pathway expression. Here we report a genetically encoded metabolic switch that enables dynamic regulation of fatty acids (FA) biosynthesis in *Escherichia coli*. The engineered strains were able to dynamically compensate the critical enzymes involved in the supply and consumption of malonyl-CoA and efficiently redirect carbon flux toward FA biosynthesis. Implementation of this metabolic control resulted in an oscillatory malonyl-CoA pattern and a balanced metabolism between cell growth and product formation, yielding 15.7- and 2.1-fold improvement in FA titer compared with the wild-type strain and the strain carrying the uncontrolled metabolic pathway. This study provides a new paradigm in metabolic engineering to control and optimize metabolic pathways facilitating the high-yield production of other malonyl-CoA–derived compounds.

biofuels | dynamic metabolic control | transcriptional regulation

A grand challenge in synthetic biology is to move the design of biomolecular circuits from purely genetic constructs toward systems that integrate different levels of cellular complexity, including regulatory networks and metabolic pathways (1). Despite the fact that a large volume of regulatory architectures and motifs has been discovered (2, 3), little has been accomplished in pathway engineering to improve cellular productivity and yield by exploiting dynamic pathway regulation and metabolic control (4). One essential part in implementing synthetic metabolic control in pathway engineering is to engineer novel metabolite sensors with desired input–output relationships. For example, Liao et al. (5–7) have designed and applied a regulatory circuit that can sense the glycolytic pathway hallmark metabolite acetyl-phosphate to control the lycopene biosynthetic pathway (5) and generate oscillatory gene expression (6) as well as achieve artificial cell–cell communication (7). Dahl et al. (8) have used stress-response promoters to improve farnesyl pyrophosphate production, and Tsao et al. (9) have rewired the *Escherichia coli* native quorum-sensing regulon for autonomous induction of recombinant proteins.

Traditional metabolic engineering is largely focused on the overexpression of rate-limiting steps (10), deletion of competing pathways (11), managing ATP (12, 13), and balancing redox and precursor metabolites (13). Although these approaches have been shown to be effective in improving cellular productivity and yield, the engineered strains are often incapable of dynamically controlling gene expression and are susceptible to environmental perturbations. For example, precursor flux improvement by overexpression of heterologous enzymes may not be accommodated by downstream pathways; the buildup of toxic intermediates may elicit stress response that compromises cell viability and pathway productivity (8, 14). On the other hand, inducible or constitutive promoters are susceptible to

environmental perturbations: any deviations from the optimal state would impair cell productivity and yield (15). Ideally, the cell would sense a critical intermediate accumulating inside the cell and trigger the expression of downstream pathways that convert this intermediate to the final product. From a control theory perspective, there is a pressing need to engineer robust cells that can automatically adjust pathway expression and adapt the metabolic activity to the changing environment (16).

Recent efforts in microbial biofuel production hinge upon constructing efficient metabolic pathways to produce a variety of fatty acids (FA)-based fuels (17–23). To date, most of the work has taken a static perspective to coordinate the expression of enzymes and optimize production titer and yield, including modification of plasmid copy number (24), promoter strength (25, 26), and combinations of these strategies (21, 27). Further production improvement calls for novel approaches that rewire transcriptional control mechanisms and achieve dynamic pathway regulation. Here we present a genetically encoded metabolic switch that enables dynamic regulation of both the malonyl-CoA source pathway and the malonyl-CoA sink pathway. Engineering hybrid promoter–transcriptional regulator interactions led to the construction of two malonyl-CoA sensors that exhibit opposing transcriptional activities. Proper balancing of the transcriptional activity of the malonyl-CoA–upregulating promoter and the malonyl-CoA–downregulating promoter resulted in an integrated malonyl-CoA switch rendering bistable gene expression pattern. When this synthetic malonyl-CoA switch was implemented to

Significance

One important synthetic chemistry reaction endowed by nature is the decarboxylative carbon condensation reaction using malonyl-CoA as carbon donor. Previous metabolic engineering efforts centered on the malonyl-CoA–dependent pathway have resulted in the production of many value-added compounds. Here we mimicked the native biological systems and used a dynamic regulatory network to optimize production titers and yield. The naturally existing transcriptional regulator FapR was rewired to dynamically control gene expressions involved in the supply and consumption of malonyl-CoA. Applying this metabolic control allowed the engineered cell to dynamically regulate pathway expression and compensated the metabolic activity of critical enzymes. The synthetic malonyl-CoA switch engineered in this study opens up new venues for dynamic pathway optimization and efficient production of malonyl-CoA–derived compounds.

control fatty acids production, the engineered strain could better balance the trade-off between cell growth and product formation and demonstrated superior FA production profile.

Results and Discussion

Characterization of Malonyl-CoA Sensors. Malonyl-CoA is the rate-limiting precursor involved in the chain elongation reaction of a range of value-added pharmaceuticals and biofuels (28, 29). Development of malonyl-CoA–responsive sensors holds great promise in overcoming critical pathway limitations and optimizing production titers and yields (30). Small-molecule–responsive transcriptional factors were generally rewired to interact with the core sequence (−35 or −10 region) of a certain promoter, offering great potential for transcriptional biosensing and metabolic control (31). Based on the findings of Schujman (32, 33), FapR is a putative transcription repressor that specifically senses malonyl-CoA and regulates gene expression in the *Bacillus subtilis* fatty acids biosynthetic pathway. By incorporating the *B. subtilis* transcription factor FapR and the *cis*-regulatory element *fapO*, our previous efforts (30) have identified a T7-based malonyl-CoA sensor exhibiting malonyl-CoA–dependent transcriptional activity (Fig. 1*A*). This T7-based malonyl-CoA sensor was shown to be able to respond to a broad range of intracellular malonyl-CoA (from 0.1 to 1.1 nmol/mgDW, *SI Appendix*, Fig. S1).

Next we engineered another malonyl-CoA sensor consisting of the *E. coli* native promoter pGAP (Fig. 1*B*). This is a σ^{70}-dependent promoter that uses the *E. coli* RNA polymerase (RNAP) to initiate gene transcription (34). Surprisingly, the transcriptional activity of the pGAP-based malonyl-CoA sensor (Fig. 1*D*) was markedly different from that of the T7-based malonyl-CoA sensor (*SI Appendix*, Fig. S1). Contrary to our expectation that FapR would act as a transcriptional repressor, gene expression from the pGAP promoter was significantly increased due to the expression of FapR (Fig. 1*D*). For example, gene expression was increased almost sevenfold in the sensor construct compared with the control construct that is devoid of FapR expression (Fig. 1*C*). Gene expression in the control constructs that are devoid of FapR expression remained relatively constant at different levels of malonyl-CoA (Fig. 1*C*). This led us to hypothesize that FapR would act as a regulator that activates gene expression from pGAP promoter. Consistent with this assumption, increased malonyl-CoA resulted in decreased gene expression in pGAP promoter (Fig. 1*D*), which could be ascribed to the fact that malonyl-CoA would disrupt the FapR–pGAP–RNAP interaction and thus deactivate the gene expression. In addition, gene expression in the sensor construct was
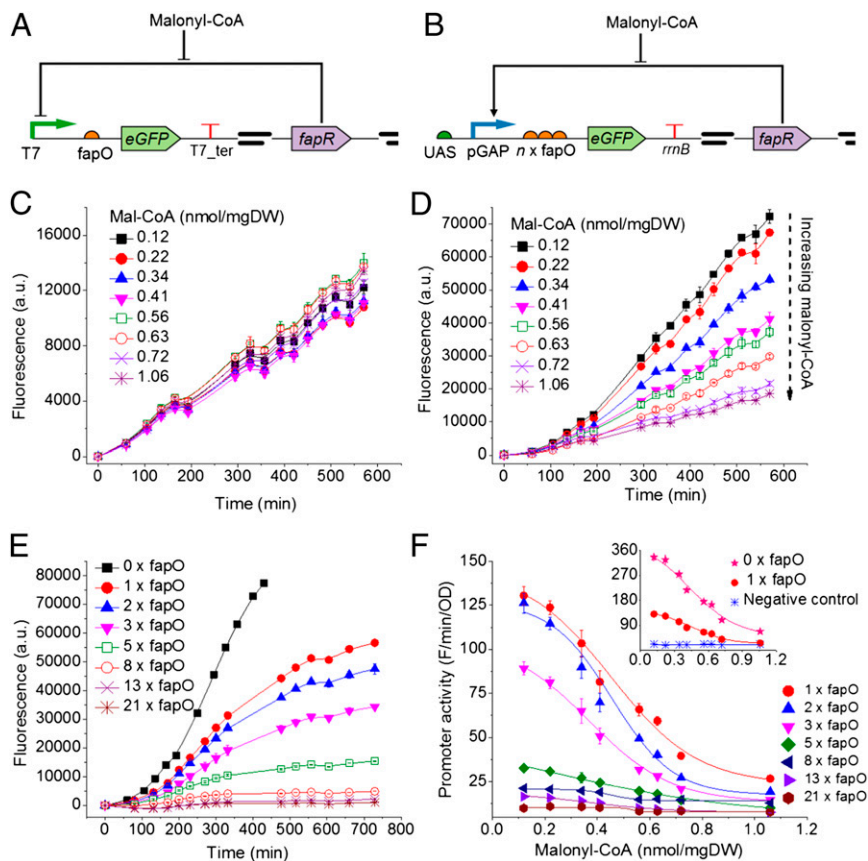
Fig. 1. Construction of malonyl-CoA sensors using dual transcriptional regulator FapR. (*A*) Structure of T7-based malonyl-CoA sensor. T7, bacteriophage T7 promoter; *fapO*, FapR repressor-binding site; eGFP, enhanced green fluorescence protein (reporter); T7_ter, T7 terminator; *fapR*, *B. subtilis* fatty acids pathway transcriptional regulator. Blunt-end arrows denote repression. (*B*) Structure of pGAP-based malonyl-CoA sensor. UAS, upstream activation sequence; pGAP, *E. coli* pGAP promoter; $n \times$ fapO, tandem copies of FapR repressor-binding site (*n* denotes the number of fapO sites); rrnB, *E. coli* transcriptional terminator. Pointed arrows indicate activation. (*C*) Gene expression from pGAP promoter that is devoid of FapR remained relatively constant at different levels of malonyl-CoA. (*D*) FapR-activated pGAP transcriptional activity was downregulated by increasing levels of malonyl-CoA. The sensor construct carries one copy of *fapO* downstream of the pGAP promoter. (*E*) Time-dependent gene expression dynamics of pGAP promoter with tandem copies of *fapO* (*n* = 0, 1, 2, 3, 5, 8, 13, and 21). (*F*) Tuning the dynamic range of pGAP-based malonyl-CoA sensor by adding different numbers of *fapO*. Malonyl-CoA deactivates the transcriptional activity of the pGAP-based sensor. Negative control is the sensor construct devoid of FapR expression.

almost restored to the level of the control construct when malonyl-CoA was increased to above 1 nmol/mgDW. We also tested the responsiveness of other *E. coli* native promoters (arabinose-induced pBAD and lactose-induced pTrc) with co-expression of FapR, but no activation effects were found in these two promoters.

Following this assumption, we turned to investigate how FapR would interact with pGAP. We arranged in tandem multiple copies of *fapO* (n = 0, 1, 2, 3, 5, 8, 13, and 21) between the pGAP promoter and the reporter gene with the expectation that increasing the number of FapR-binding sites would strengthen the transcriptional activation. Contrary to our expectations, gene expression from the pGAP promoter was decreased by increasing the number of *fapO* sites inserted onto the promoter region (Fig. 1E). This behavior could be the result of the presence of repeated sequence spacers that increased the distance of the promoter from the structural gene (35). Surprisingly, the sensor construct devoid of any FapR-binding site (n = 0, Fig. 1E) exhibited the strongest gene activation, leading us to hypothesize that FapR binds with the pGAP at a region other than the *fapo* site. Naturally, we opted to search for possible FapR-binding sites within the adjacent region of pGAP promoter. The pGAP promoter, which carries multiple transcriptional factor-binding sites, confers on *E. coli* the ability to produce high levels of the essential glycolysis enzyme glyceraldehyde-3-phosphate dehydrogenase under various growth conditions (36). Using a computational toolbox that predicts transcriptional factor-binding sites (37), we identified an activation sequence upstream of the pGAP promoter that could potentially interact with FapR. To physically validate that FapR interacts with this upstream activation sequence (UAS), we performed Surface Plasmon Resonance (SPR) analysis (38, 39) with purified FapR protein and biotinylated synthetic oligos (*fapO* and UAS) as testing subjects (*SI Appendix*, Figs. S2 and S3). SPR analysis revealed that FapR has a comparable binding affinity toward UAS (K_D =

7.2×10^{-7} M) as opposed to the binding affinity between FapR and *fapO* (1.2×10^{-7} M) (*SI Appendix*, Table S1). Deletion of this UAS sequence completely eliminated the transcriptional activation (*SI Appendix*, Fig. S4), thus confirming our assumption that FapR binds with UAS sequence and activates gene expression from pGAP promoter.

Precise control and regulation of heterologous pathway expression requires the engineering of molecular sensors that span across a wide range of gene expression dynamics. Generally, the desired transcriptional dynamics could be tuned by engineering transcriptional factor and promoter interactions (40). By incorporating different copy numbers of *fapO*, the absolute promoter activity of the pGAP promoter was decreased by 35-fold from 350 F/min/OD in the sensor with no *fapO* sites (n = 0) to 10 F/min/OD in the sensor with 21 copies of *fapO* (n = 21) (Fig. 1F). All of the sensors exhibited malonyl-CoA–dependent transcriptional activity with increased malonyl-CoA leading to decreased promoter activity. These finely tuned malonyl-CoA sensors paved the way for implementing synthetic metabolic controls and optimizing the production of malonyl-CoA–derived compounds.

Switching Properties of Integrated Malonyl-CoA Sensors. One central goal of synthetic biology is to integrate multiple gene circuits and achieve dynamic control in living biological systems (41, 42). The signal-processing capability of integrated circuits is closely related with the regulatory architecture and dynamics of the composed circuits (43). As such, integrated synthetic gene circuits often cannot work properly due to various design faults. For example, the use of multiple regulators/promoters tends to result in circuits with mismatched gene expression levels, incoherent input signal ranges, and delayed time response curves (43, 44). A functional integrated circuit will require extensive work to iteratively tune the responsiveness of the interacting molecules.

By integrating the malonyl-CoA–regulated T7 and pGAP promoter, we demonstrated that gene expression of two reporter proteins (eGFP and mCherry) can be exclusively switched between two distinct states depending on the intracellular level of malonyl-CoA (Fig. 2). When the level of malonyl-CoA was low, FapR activated gene expression from the pGAP promoter and led to increased eGFP signal. At the same time, FapR repressed gene expression from the T7 promoter and led to a relatively lower mCherry signal. On the other hand, when the level of malonyl-CoA was high, malonyl-CoA changed the DNA-binding affinity of FapR and thus destabilized the transcriptional complex comprising FapR, RNA polymerase, and the interacting promoters (Fig. 2A). As a result, eGFP expression from pGAP promoter was deactivated and mCherry expression from the T7 promoter was derepressed, leading to a flip-flopped expression of eGFP and mCherry (Fig. 2C). When different numbers of FapR-binding sites (*fapO*) were inserted into the pGAP-based circuits (Fig. 2 B–D), gene expression from the integrated circuits created different switching properties. For example, pGAP promoter with none (n = 0, Fig. 2B), one (n = 1, Fig. 2C), and three (n = 3, Fig. 2D) copies of *fapO* exhibited around 112, 43, and 20% relative promoter activity, respectively, when the T7 promoter switched to half its saturation activity (intracellular malonyl-CoA concentration is around 0.6 nmol/mgDW).

In contrast to cross-regulation and toggle switches that use mutually repressible promoters to control gene expression, the malonyl-CoA switch constructed in this study was composed of a single regulatory protein (FapR) controlling the expression of two different promoters (T7 and pGAP) that are transcribed by different RNA polymerases (T7 RNAP and *E. coli* RNAP). The advantage of using a single regulatory protein is that the time responsiveness and robustness of the system can be improved and therefore the trivial tweaking and twisting work that is often required to ensure a functional circuit can be avoided. These fine-tuned gene-expression switching properties should facilitate
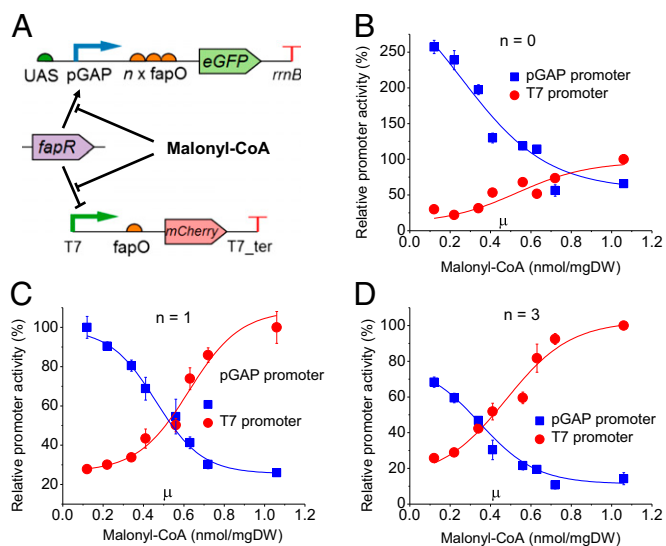
Fig. 2. Gene expression switching properties of integrated malonyl-CoA sensors. (A) Schematic representation of the engineered malonyl-CoA switches consisting of two reporter genes under the control of T7 promoter and pGAP promoter. Symbols are the same as the symbols in Fig. 1. (B–D) Switching property of the integrated malonyl-CoA circuits with a different number of FapR-binding sites (B, n = 0; C, n = 1; D, n = 3). The pGAP relative promoter activity is calculated based on the promoter activity of each circuit (n = 0, n = 1, and n = 3) with respect to the saturation promoter activity of the circuit with one copy of *fapO* (n = 1). Smooth curves represent dose–response fitting of the scattered data points.
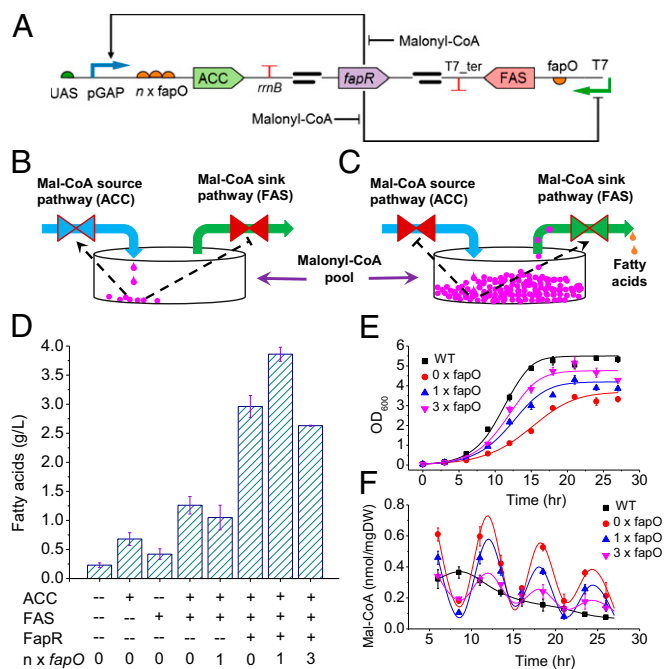
Fig. 3. Dynamic pathway control to improve fatty acids production. (*A*) Molecular structure of the constructed malonyl-CoA controller. Malonyl-CoA source pathway (ACC, encoded by *accADBC*) was under the control of malonyl-CoA–downregulated pGAP promoter; malonyl-CoA sink pathway (FAS, encoded by *fabADGI* and *tesA'*) was under the control of malonyl-CoA–upregulated T7 promoter. Other symbols are the same as the symbols in Fig. 1. (*B*) Low level of malonyl-CoA switches on the expression of malonyl-CoA source pathway (ACC) and switches off the expression of the malonyl-CoA sink pathway (FAS). (*C*) High level of malonyl-CoA switches off the expression of the malonyl-CoA source pathway (ACC) and switches on the expression of the malonyl-CoA sink pathway (FAS). (*D*) Implementing dynamic malonyl-CoA control to improve fatty acids production. The first column represents the wild-type strain. All other strains (columns 2–8) carry a chromosomal mutant version of *fad*D encoding the fatty acyl-CoA synthetase. The last three columns represent strains carrying the controlled FA biosynthetic pathway with different numbers of the FapR repressor-binding site regulating the malonyl-CoA source (ACC) pathway. "*n* × fapO" denotes the number of *fapO* within pGAP-based circuits (*n* = 0, 1, and 3). (*E*) Cell growth curve in the strains carrying the uncontrolled FA biosynthetic pathway (wild-type strain) and the controlled FA biosynthetic pathway (*n* = 0, 1, and 3). Smooth curves represent logistic fitting of the scattered data points. (*F*) Intracellular malonyl-CoA profile in the strains carrying the uncontrolled FA biosynthetic pathway (wild-type strain) and the controlled FA biosynthetic pathway (*n* = 0, 1, and 3).

the construction of strains with controlled expression of important metabolic pathways and efficient biosynthesis of malonyl-CoA–derived compounds.

Dynamic Pathway Regulation to Improve Fatty Acids Production. We next sought to implement this malonyl-CoA–dependent metabolic switch to control and optimize fatty acids biosynthesis in *E. coli*. For this purpose, the malonyl-CoA source pathway (acetyl-CoA carboxylase, encoded by *accADBC*) was placed under the control of the pGAP promoter and malonyl-CoA sink pathway (fatty acids synthase, encoded by *fabADGI* and *tesA'*) was placed under the control of the T7 promoter (Fig. 3*A*). When malonyl-CoA level is low, FapR activates the transcription of the malonyl-CoA source pathway and represses the transcription of the malonyl-CoA sink pathway. As a result, malonyl-CoA is expected to accumulate inside the cell (Fig. 3*B*). On the other hand, when malonyl-CoA reaches a critical concentration, binding of malonyl-CoA to FapR increases the possibility of

FapR dissociation from the interacting promoters. Consequently, transcription of the malonyl-CoA source pathway [acetyl-CoA carboxylase (ACC)] will be turned off and transcription of the malonyl-CoA sink pathway [fatty acids synthase (FAS)] will be turned on, leading to increased expression of the malonyl-CoA sink pathway that converts the accumulated malonyl-CoA to fatty acids (Fig. 3*C*).

To validate the above-mentioned control scheme, we experimentally interfaced the synthetic malonyl-CoA switch with the fatty acids biosynthetic pathway and investigated whether the proposed control scheme would improve fatty acids production. Overexpression of either ACC (second column, Fig. 3*D*) or FAS (third column, Fig. 3*D*) pathway led to strains producing around 0.68 and 0.42 g/L of fatty acids, respectively, a 196 and 82.6% increase compared with the *E. coli* BL21 wild-type strain (first column, Fig. 3*D*). Coupled expression of the malonyl-CoA source pathway ACC and the malonyl-CoA sink pathway FAS (fourth column, Fig. 3*D*) further increased the fatty acids to 1.26 g/L. Insertion of one copy of *fapO* regulating the ACC pathway (fifth column, Fig. 3*D*) moderately decreased the fatty acids production, possibly due to the decreased transcriptional activity of the pGAP promoter when *fapO* was incorporated (Fig. 1*E*). The strains engineered with FapR regulating both the malonyl-CoA source pathway (ACC) and the malonyl-CoA sink pathway (FAS) (sixth, seventh, and eighth columns, Fig. 3*D*) demonstrated remarkably increased fatty acids production compared with the strains carrying the uncontrolled ACC and FAS pathway (fourth column, Fig. 3*D*). For example, the controlled ACC and FAS pathway produced around 2.96, 3.86, and 2.63 g/L of fatty acids, respectively, when none (*n* = 0, sixth column, Fig. 3*D*), one (*n* = 1, seventh column, Fig. 3*D*), and three (*n* = 3, eighth column, Fig. 3*D*) copies of *fapO* were used to regulate the malonyl-CoA source pathway, representing a 1.3, 2.1, and 1.1-fold increase compared with the uncontrolled metabolic pathway (fourth column, Fig. 3*D*). The yield (0.20 g fatty acids/g glucose, 56% of the theoretical yield of the FA pathway) is comparable with the highest yield (0.28 g fatty acids/g glucose, 52.4% of the theoretical yield of the β-oxidation reversal pathway) ever reported (*SI Appendix*, Table S2). Due to the expression of cytosolic thioesterase (TesA'), a significant amount of the carbon flux was redirected to the biosynthesis of the medium-chain myristic acid (C14:0) in the engineered strains (*SI Appendix*, Fig. S5). To elucidate how the synthetic malonyl-CoA switch regulates the fatty acids biosynthesis, we examined cell growth (Fig. 3*E*) and intracellular malonyl-CoA (Fig. 3*F*) in the wild-type strains and the engineered strains with different numbers of *fapO* sites (*n* = 0, 1, and 3). Not surprisingly, strains with the controlled FA biosynthetic pathway suffered from a low-cell-growth rate (0.32 h^{-1} for *n* = 0, 0.41 h^{-1} for *n* = 1, and 0.45 h^{-1} for *n* = 3) compared with the wild-type strain (0.49 h^{-1}). This largely could be ascribed to the effects of stress, that is, the expression of heterologous proteins that deprive essential cellular resources for maintaining the normal growth rate. When no *fapO* was used (*n* = 0), both the pGAP promoter and the T7 promoter exhibited relatively higher transcriptional activity (Fig. 2*B*), leading to increased expression of ACC and FAS. As a result, the cell growth rate was reduced by 35% from 0.49 to 0.32 h^{-1}.

Interestingly, intracellular malonyl-CoA exhibited an oscillatory changing pattern in the strains carrying the synthetic malonyl-CoA controller (Fig. 3*F*), compared with that of the wild-type strain exhibiting a monotonic decrease at the exponential and stationary phases. The decreased amplitude of the oscillation indicates the reduced regulating capability of the malonyl-CoA switch, possibly due to the inhibitory effects associated with the accumulation of fatty acids and toxic by-products. The highest fatty acids production was obtained in the strains with only one copy of *fapO* regulating the ACC pathway (seventh column, Fig. 3*D*), indicating that strains with moderately

oscillating malonyl-CoA pattern (Fig. 3*E*) could better manage the trade-off between cell growth and heterologous pathway expression. Due to the dynamic nature of this system, the "on" and "off" state of the ACC pathway and the FAS pathway must be switched at the right time such that the malonyl-CoA consumed by FAS could be efficiently replenished by ACC, and the malonyl-CoA generated by ACC can be efficiently consumed by FAS. Not surprisingly, switching the expression of ACC to FAS too late ($n = 0$) and too early ($n = 3$) resulted in relatively strong and weak malonyl-CoA oscillation and suboptimal fatty acids production (Figs. 2 and 3*F*). These results demonstrate that the engineered strains can dynamically regulate the expression of both the malonyl-CoA source pathway and the malonyl-CoA sink pathway and efficiently redirect carbon flux toward FA biosynthesis.

Conclusions. One important synthetic chemistry reaction endowed by nature is the decarboxylative carbon condensation reaction using malonyl-CoA as carbon donor (29). Previous metabolic engineering efforts centered on malonyl-CoA–dependent pathways have resulted in the production of many value-added compounds including fatty acids (21), phenylpropanoids (45, 46), and polyketides (47). Here we mimicked the native biological systems and used a dynamic regulatory network to optimize production titers and yield. In the present work, the naturally existing transcriptional regulator FapR was rewired to control the FA biosynthetic pathway of *E. coli*. Optimal control of gene expression involved in the supply and consumption of malonyl-CoA resulted in balanced metabolism between cell growth and product formation and significantly improved fatty acids production. Applying this metabolic control allowed the engineered cell to dynamically regulate pathway expression and compensated the metabolic activity of critical enzymes based on the intracellular level of malonyl-CoA. The synthetic malonyl-CoA switch engineered in this study opens up new venues for dynamic pathway optimization and efficient production of malonyl-CoA–derived compounds.

Materials and Methods

Malonyl-CoA Sensor Construction. Synthetic gene fragment fapO-eGFP, codon-optimized *fapR*, *Discosoma sp* mCherry, and custom-designed pGAP-ePath (*SI Appendix*, Table S6–S9) were synthesized from IDT or GenScript. pOM vector was a gift by Dr. T. Hueller from Evonik Degussa GmbH (Creavis Technologies & Innovation, Marl, Germany) (*SI Appendix*, Table S5). To construct T7-based malonyl-CoA sensor, eGFP or fapO-eGFP were cloned into vector pETM9 (30) to give construct pETM9-eGFP or pETM9-fapO-eGFP. mCherry was inserted into pETM9-fapO-eGFP in place of eGFP to give pETM9-fapO-mCherry. Then the fapO-mCherry gene fragment from pETM9-fapO-mCherry was cloned into pCDM4 using restriction sites AvrII and KpnI to give construct pCDM4-fapO-mCherry. Codon-optimized *fapR* was subcloned into pACM4 and pCDM4 using restriction sites NdeI and XhoI to give construct pACM4-fapR and pCDM4-fapR.

To construct the pGAP-based malonyl-CoA sensor, eGFP from pIDTBlue-fapO-eGFP was subcloned into pOM to give pOM-0×fapO-eGFP using restriction sites XbaI and HindIII. Then fapO-eGFP was subcloned into pBAD24 using restriction sites NheI and HindIII to give pBAD24-1×fapO-eGFP. Due to the internal XbaI site in front of eGFP, multiple copies of *fapO* were inserted by iteratively ligating the XbaI/HindIII-digested recipient vector (i.e., pBAD24-m×fapO-eGFP) and the NheI/HindIII-digested donor vector (i.e., pBAD24-n×fapO-eGFP) to give the construct pBAD24-(m+n)×fapO-eGFP. Then the n×fapO-eGFP gene fragment from pBAD24-n×fapO-eGFP was subcloned into pOM to give pOM-n×fapO-eGFP ($n = 0, 1, 2, 3, 5, 8, 13$, and 21) using restriction sites NheI/HindIII and XbaI/HindIII. To eliminate the UAS sequence, an additional SalI site in front of the pGAP promoter was inserted into pOM-fapO-eGFP by Quickchange II site-directed mutagenesis kits using primer pairs SalI_pOMF and SalI_pOMR. Then the SalI single-digested pOM-fapO-eGFP was self-ligated to give construct pOM0-fapO-eGFP. All clones were screened by restriction digestion analysis and verified by gene sequencing.

FAS and ACC Pathway Construction. To construct FAS pathway, *E. coli* tesA', *fabA*, *fabD*, *fabG*, and *fabI* gene fragments were assembled into artificial operon form based on the ePathBrick gene assembly platform (48). Briefly,

the XbaI/SalI-digested donor vector was ligated to the SpeI/SalI-digested recipient vector to give an operon gene configuration. The resulting synthetic operon containing *tesA'-fabADGI* was cloned into pETM9-fapO-eGFP in place of eGFP with an XbaI/SalI digest. Then, the *tesA'-fabADGI* gene fragment from pETM9-fapO-FAS was cloned into pRSM3 vector to give pRSM4-fapO-FAS using restriction sites AvrII and SalI.

The synthetic gene fragment containing UAS, pGAP promoter, ePathBrick restriction sites, and *rrnB* terminator (*SI Appendix*, Table S9) was cloned into pETM6 to give pXPA vector using restriction sites ApaI and SalI. Then eGFP, 1×fapO-eGFP, and 3×fapO-eGFP from pBAD24-n×fapO-eGFP ($n = 0, 1$, and 3) were subcloned into pXPA vector using restriction sites XbaI/KpnI and NheI/KpnI, yielding vectors pXPA-eGFP, pXPA-1×fapO-eGFP, and pXPA-3×fapO-eGFP. To construct the ACC pathway, *E. coli accA, accD, accB*, and *accC* gene fragments were assembled into an artificial operon form based on the ePathBrick gene assembly platform (48). Next, the eGFP fragment in pXPA-eGFP, pXPA-1×fapO-eGFP, and pXPA-3×fapO-eGFP was replaced by the synthetic operon containing accADBC with an XbaI/SalI digest, yielding vectors pXPA-ACC, pXPA-1×fapO-ACC, and pXPA-3×fapO-ACC, respectively. All clones were screened by restriction digestion analysis and verified by gene sequencing.

Sensor Activity Assay. Fluorescence intensity was used to characterize the promoter activity among the engineered sensors. Host cell BL21*(DE3) transformed with different sensor plasmids was grown overnight in LB at 37 °C and $250 \times g$. The next morning, 10 mL fresh LB was inoculated with 8% (vol/vol) overnight culture in 50-mL Corning tubes and grown at 37 °C with shaking at $250 \times g$ for ~1 h (OD of 0.2 in a 96-well plate). Cell culture (240 μL) was transferred to a Greiner Bio-one 96-well fluorescence plate (Bio-Greiner). Different amounts of isopropyl β-D-1-thiogalactopyranoside (IPTG) and cerulenin were added to the cell culture to induce the expression of FapR and stimulate the level of malonyl-CoA. The fluorescence plates were covered and sealed with parafilm to prevent evaporation. Cells were left to grow at 37 °C with shaking at $300 \times g$ on a benchtop plate shaker (Labnet VorTemp 56 shaker incubator). Cell optical density and expression of fluorescence protein (eGFP and mCherry) were simultaneously detected every 30 or 45 min using a Biotek Synergy 4 microplate reader. Optical density was read at 600 nm. For measurement of only eGFP signal, a Tungsten light source with monochrome filter (excitation: 485 ± 20 nm; emission: 528 ± 20 nm) was used. For measurement of both eGFP and mCherry, Xenon light source was used; the excitation and emission wavelength settings for eGFP and mCherry were 470/510 and 580/620 nm, respectively. All experiments were performed in triplicates.

Fatty Acids Fed-Batch Fermentation. Fed-batch scale fermentation was performed with a 2-L stirred tank bioreactor. Fresh cells from agar plates were used to inoculate 50 mL MK media [13.5 g/L KH$_2$PO$_4$, 4.0 g/L (NH$_4$)$_2$HPO$_4$, 1.7 g/L citric acid, 20 g/L glucose, 10 g/L yeast extract, and 10 mL/L trace metals (21) with pH adjusted to 6.8 by sodium hydroxide] with appropriate antibiotics in 250-mL shake flasks and allowed to grow at 37 °C for 20 h. Exponentially growing cells from the overnight culture were inoculated to the bioreactor containing 1.2 L of MK media with an initial OD of 0.08. The bioreactor was run at a fixed oxygen concentration (30% saturation) and 37 °C with aeration rate at 1.5 vvm. Induction of FapR expression was performed by adding 100 μM IPTG, and the cultivation temperature was switched to 33 °C at 6 h of fermentation (OD = 5). Ten milliliters of 40% glucose was pulsed into the bioreactor at 20 and 32 h after the start of the fermentation. Samples were taken at the end of the fermentation (44 h) and subjected to fatty acids extraction and analysis. Bioreactor experiments were performed in duplicates.

Fatty Acids and Malonyl-CoA Quantification. Total fatty acids were extracted using a modified protocol reported by Voelker (49). Briefly, 0.4 mL of culture was acidified with 40 μL of acetic acid, spiked with 5 μL of 10 mg/mL pentadecanoic acid as an internal standard, and partitioned with 750 μL of CHCl$_3$-CH$_3$OH (2:1 by volume) at room temperature. The extraction was performed with a VWR high-duty vortex platform at $1,600 \times g$ for 1 h. After a brief centrifugation, 400 μL of lower-phase chloroform was transferred to Eppendorf tubes and evaporated to dryness with a Vacufuge. The resulting crude fatty acids were redissolved in 400 μL 5% (vol/vol) H$_2$SO$_4$ in methanol and incubated in a sealed vial at 60 °C for 2 h. Four hundred microliters of 0.9% NaCl was added to the reaction mixture, and the resulting fatty acid methyl esters (FAMEs) were extracted with 250 μL of hexane. Gas chromatography analysis of FAMEs was performed with a Bruker GC-450 equipped with a Flame ionization detector and a capillary column HP-INNOWAX (30 m × 0.25 mm), following the procedures reported by Tai (10).

For malonyl-CoA quantification, *E. coli* cell culture (around 40 OD units) was chilled in ice and centrifuged at $4,500 \times g$ and 4 °C for 15 min. Cell pellet

was then frozen with liquid nitrogen and homogenized with mortar and pestle in 2.0 mL 6% prechilled perchloric acid supplemented with 0.5 μg/mL [^{13}C$_3$]-malonyl-CoA as internal standard. After centrifugation at 4,500 × g and 4 °C for 15 min, the supernatant was loaded to a Waters solid-phase extraction column to remove salt and concentrate malonyl-CoA. Then the elute was subjected to liquid chromatography–mass spectrometry analysis to determine the intracellular levels of malonyl-CoA following the procedure described by Onorato (50).

1. Oyarzún DA, Stan G-BV (2012) Synthetic gene circuits for metabolic control: Design trade-offs and constraints. *J R Soc Interface* 10(78), 10.1098/rsif.2012.0671.
2. Milo R, et al. (2002) Network motifs: Simple building blocks of complex networks. *Science* 298(5594):824–827.
3. Chubukov V, Zuleta IA, Li H (2012) Regulatory architecture determines optimal regulation of gene expression in metabolic pathways. *Proc Natl Acad Sci USA* 109(13):5127–5132.
4. Afroz T, Beisel CL (2013) Understanding and exploiting feedback in synthetic biology. *Chem Eng Sci* 103(0):79–90.
5. Farmer WR, Liao JC (2000) Improving lycopene production in Escherichia coli by engineering metabolic control. *Nat Biotechnol* 18(5):533–537.
6. Fung E, et al. (2005) A synthetic gene-metabolic oscillator. *Nature* 435(7038):118–122.
7. Bulter T, et al. (2004) Design of artificial cell-cell communication using gene and metabolic networks. *Proc Natl Acad Sci USA* 101(8):2299–2304.
8. Dahl RH, et al. (2013) Engineering dynamic pathway regulation using stress-response promoters. *Nat Biotechnol* 31(11):1039–1046.
9. Tsao C-Y, Hooshangi S, Wu H-C, Valdes JJ, Bentley WE (2010) Autonomous induction of recombinant proteins by minimally rewiring native quorum sensing regulon of E. coli. *Metab Eng* 12(3):291–297.
10. Tai M, Stephanopoulos G (2013) Engineering the push and pull of lipid biosynthesis in oleaginous yeast Yarrowia lipolytica for biofuel production. *Metab Eng* 15(1):1–9.
11. Stephanopoulos G (2012) Synthetic biology and metabolic engineering. *ACS Synth Biol* 1(11):514–525.
12. Lan EI, Liao JC (2012) ATP drives direct photosynthetic production of 1-butanol in cyanobacteria. *Proc Natl Acad Sci USA* 109(16):6018–6023.
13. Singh A, Cher Soh K, Hatzimanikatis V, Gill RT (2011) Manipulating redox and ATP balancing for improved production of succinate in E. coli. *Metab Eng* 13(1):76–81.
14. Leonard E, et al. (2010) Combining metabolic and protein engineering of a terpenoid biosynthetic pathway for overproduction and selectivity control. *Proc Natl Acad Sci USA* 107(31):13654–13659.
15. Zhang F, Carothers JM, Keasling JD (2012) Design of a dynamic sensor-regulator system for production of chemicals and fuels derived from fatty acids. *Nat Biotechnol* 30(4):354–359.
16. Dunlop MJ, Keasling JD, Mukhopadhyay A (2010) A model for improving microbial biofuel production using a synthetic feedback loop. *Syst Synth Biol* 4(2):95–104.
17. Blazeck J, et al. (2014) Harnessing Yarrowia lipolytica lipogenesis to create a platform for lipid and biofuel production. *Nat Commun* 5:3131.
18. Dellomonaco C, Clomburg JM, Miller EN, Gonzalez R (2011) Engineered reversal of the β-oxidation cycle for the synthesis of fuels and chemicals. *Nature* 476(7360):355–359.
19. Choi YJ, Lee SY (2013) Microbial production of short-chain alkanes. *Nature* 502(7472):571–574.
20. Howard TP, et al. (2013) Synthesis of customized petroleum-replica fuel molecules by targeted modification of free fatty acid pools in Escherichia coli. *Proc Natl Acad Sci USA* 110(19):7636–7641.
21. Xu P, et al. (2013) Modular optimization of multi-gene pathways for fatty acids production in E. coli. *Nat Commun* 4:1409.
22. Tee TW, Chowdhury A, Maranas CD, Shanks JV (2014) Systems metabolic engineering design: Fatty acid production as an emerging case study. *Biotechnol Bioeng* 111(5):849–857.
23. Xiong M, et al. (2012) A bio-catalytic approach to aliphatic ketones. *Sci Rep* 2:311.
24. Juminaga D, et al. (2012) Modular engineering of L-tyrosine production in Escherichia coli. *Appl Environ Microbiol* 78(1):89–98.
25. Anthony JR, et al. (2009) Optimization of the mevalonate-based isoprenoid biosynthetic pathway in Escherichia coli for production of the anti-malarial drug precursor amorpha-4,11-diene. *Metab Eng* 11(1):13–19.
26. Du J, Yuan Y, Si T, Lian J, Zhao H (2012) Customized optimization of metabolic pathways by combinatorial transcriptional engineering. *Nucleic Acids Res* 40(18):e142.
27. Ajikumar PK, et al. (2010) Isoprenoid pathway optimization for Taxol precursor overproduction in Escherichia coli. *Science* 330(6000):70–74.
28. Xu P, Ranganathan S, Fowler ZL, Maranas CD, Koffas MA (2011) Genome-scale metabolic network modeling results in minimal interventions that cooperatively force carbon flux towards malonyl-CoA. *Metab Eng* 13(5):578–587.
29. Felnagle EA, Chaubey A, Noey EL, Houk KN, Liao JC (2012) Engineering synthetic recursive pathways to generate non-natural small molecules. *Nat Chem Biol* 8(6):518–526.
30. Xu P, et al. (2014) Design and kinetic analysis of a hybrid promoter-regulator system for malonyl-CoA sensing in Escherichia coli. *ACS Chem Biol* 9(2):451–458.
31. Cox RS III, Surette MG, Elowitz MB (2007) Programming gene expression with combinatorial promoters. *Mol Syst Biol* 3(1):145.
32. Schujman GE, Paoletti L, Grossman AD, de Mendoza D (2003) FapR, a bacterial transcription factor involved in global regulation of membrane lipid biosynthesis. *Dev Cell* 4(5):663–672.
33. Schujman GE, et al. (2006) Structural basis of lipid biosynthesis regulation in Gram-positive bacteria. *EMBO J* 25(17):4074–4083.
34. Singh SS, Typas A, Hengge R, Grainger DC (2011) Escherichia coli σ70 senses sequence and conformation of the promoter spacer region. *Nucleic Acids Res* 39(12):5109–5118.
35. Egbert RG, Klavins E (2012) Fine-tuning gene networks using simple sequence repeats. *Proc Natl Acad Sci USA* 109(42):16817–16822.
36. Thouvenot B, Charpentier B, Branlant C (2004) The strong efficiency of the Escherichia coli gapA P1 promoter depends on a complex combination of functional determinants. *Biochem J* 383(Pt 2):371–382.
37. Tompa M, et al. (2005) Assessing computational tools for the discovery of transcription factor binding sites. *Nat Biotechnol* 23(1):137–144.
38. Szabo A, Stolz L, Granzow R (1995) Surface plasmon resonance and its use in biomolecular interaction analysis (BIA). *Curr Opin Struct Biol* 5(5):699–705.
39. Pattnaik P (2005) Surface plasmon resonance: Applications in understanding receptor-ligand interaction. *Appl Biochem Biotechnol* 126(2):79–92.
40. Ang J, Harris E, Hussey BJ, Kil R, McMillen DR (2013) Tuning response curves for synthetic biology. *ACS Synth Biol* 2(10):547–567.
41. Daniel R, Rubens JR, Sarpeshkar R, Lu TK (2013) Synthetic analog computation in living cells. *Nature* 497(7451):619–623.
42. Moon TS, Lou C, Tamsir A, Stanton BC, Voigt CA (2012) Genetic programs constructed from layered logic gates in single cells. *Nature* 491(7423):249–253.
43. Nandagopal N, Elowitz MB (2011) Synthetic biology: Integrated gene circuits. *Science* 333(6047):1244–1248.
44. Cheng AA, Lu TK (2012) Synthetic biology: An emerging engineering discipline. *Annu Rev Biomed Eng* 14:155–178.
45. Lim CG, Fowler ZL, Hueller T, Schaffer S, Koffas MA (2011) High-yield resveratrol production in engineered Escherichia coli. *Appl Environ Microbiol* 77(10):3451–3460.
46. Lin Y, Shen X, Yuan Q, Yan Y (2013) Microbial biosynthesis of the anticoagulant precursor 4-hydroxycoumarin. *Nat Commun* 4:2603.
47. Ma SM, et al. (2009) Complete reconstitution of a highly reducing iterative polyketide synthase. *Science* 326(5952):589–592.
48. Xu P, Vansiri A, Bhan N, Koffas MA (2012) ePathBrick: A synthetic biology platform for engineering metabolic pathways in E. coli. *ACS Synth Biol* 1(7):256–266.
49. Voelker TA, Davies HM (1994) Alteration of the specificity and regulation of fatty acid synthesis of Escherichia coli by expression of a plant medium-chain acyl-acyl carrier protein thioesterase. *J Bacteriol* 176(23):7320–7327.
50. Onorato JM, et al. (2010) Liquid-liquid extraction coupled with LC/MS/MS for monitoring of malonyl-CoA in rat brain tissue. *Anal Bioanal Chem* 397(7):3137–3142.